Supporting Information

Electrochemical production of hydrogen peroxide by non-noble metal-doped g-C_3N_4 under neutral electrolyte

Ying Wang,[#] Hongcen Yang,[#] Niandi Lu, Di Wang, Kun Zhu, Zhixia Wang, Lianshan Mou,Yan Zhang, Yawei Zhao, Fei Ma,* Shanglong Peng.*

School of Physical Science and Technology, School of Materials and Energy, Lanzhou University, Lanzhou 730000, China

*Corresponding author. E-mail: pengshl@lzu.edu.cn; maf@lzu.edu.cn

Figure S1. XPS full spectra of CNNs, K/ CNNs, Co/CNNs and K-Co/CNNs.

Figure S2. (A) K 2p and (B) Co 2p XPS spectra of K/CNNs, Co/ CNNs and K-Co/CNNs.

Figure S3. (A) (B) (C) (D) CV curve of CNNs, K/ CNNs, Co/ CNNs, K-CO / CNNs.

Figure S4. The different Co contents of the (A) LSV curve, (B) production rate of H_2O_2, (C) electron transfer number, (D) Faraday efficiency.

Figure S5. The different K contents of the (A) LSV curve, (B) production rate of H_2O_2, (C) electron transfer number, (D) Faraday efficiency.

Figure S6. (A) CdI curve of CNNS, K/CNNS, Co/CNNS, K-CO /CNNS. (B) the accumulation of H_2O_2 within 24 hours of K-CO /CNNS.

Figure S7. CNNs, K/CNNs, Co/CNNs and K-Co/CNNs of the (A) Comparison of N_2 adsorption and desorption curves, (B) Comparison of BET specific surface area.

Figure S8. (A)The absorption spectra of different concentrations of $Ce(SO_4)_2$, (B) the linear relationship between the concentration of $Ce(SO_4)_2$ and the absorbance.

Figure S9. Tafel plots of CNNS, K/CNNS, Co/CNNs, K-Co/CNNs.

Figure S10. (A) Structural diagram of CNNs, (B) Structural diagram of Co/CNNs, (C) Structural diagram of K/CNNs.

Figure S11. (A) Structure of CNNs for H_2O_2 adsorption, (B) Structure of Co/CNNs for H_2O_2 adsorption, (C) Structure of K/CNNs for H_2O_2 adsorption.

Table S1. The comparisons of different electrocatalysts towards two-electron ORR to produce H2O2.

Table S2. Comparison of direct anthraquinone and oxygen reduction reaction methods for the preparation of H_2O_2.

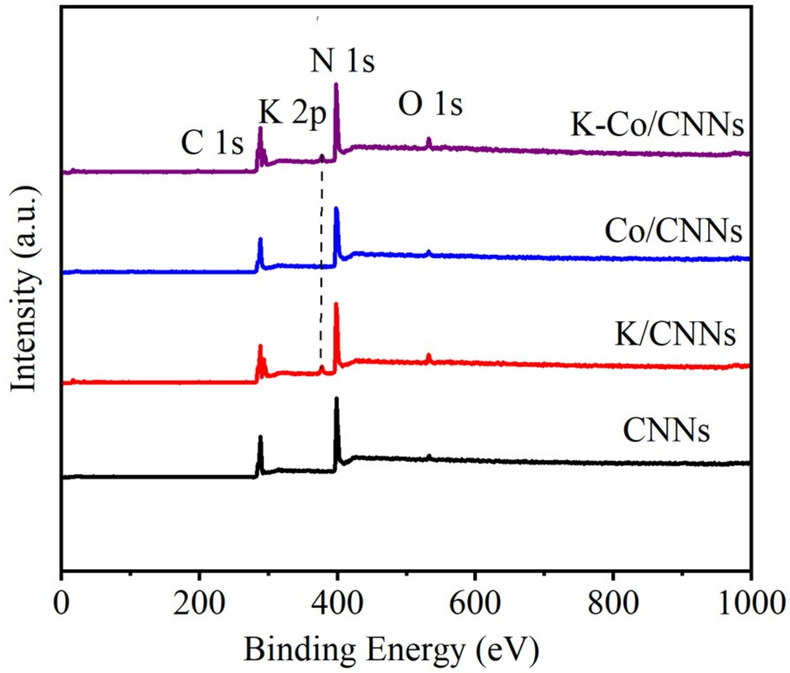

Figure S1. XPS full spectra of CNNs, K/ CNNs, Co/CNNs and K-Co/CNNs.

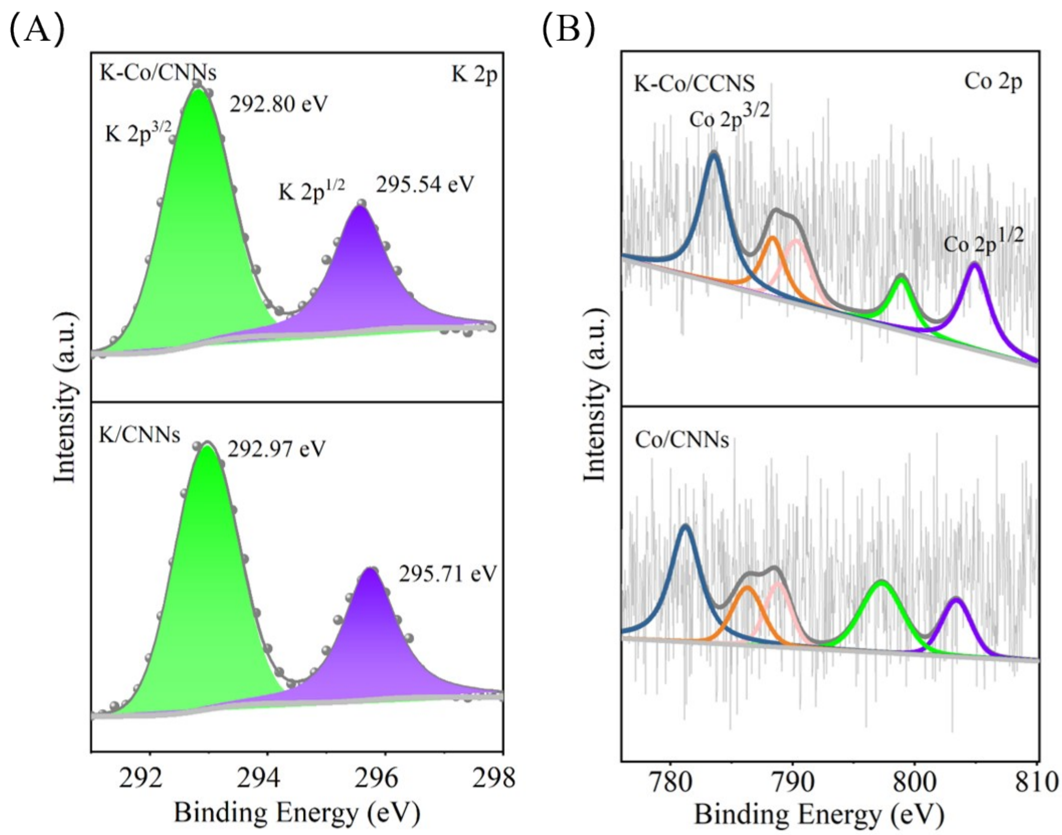

Figure S2. (A) K 2p and (B) Co 2p XPS spectra of K/CNNs, Co/ CNNs and K-Co/CNNs.

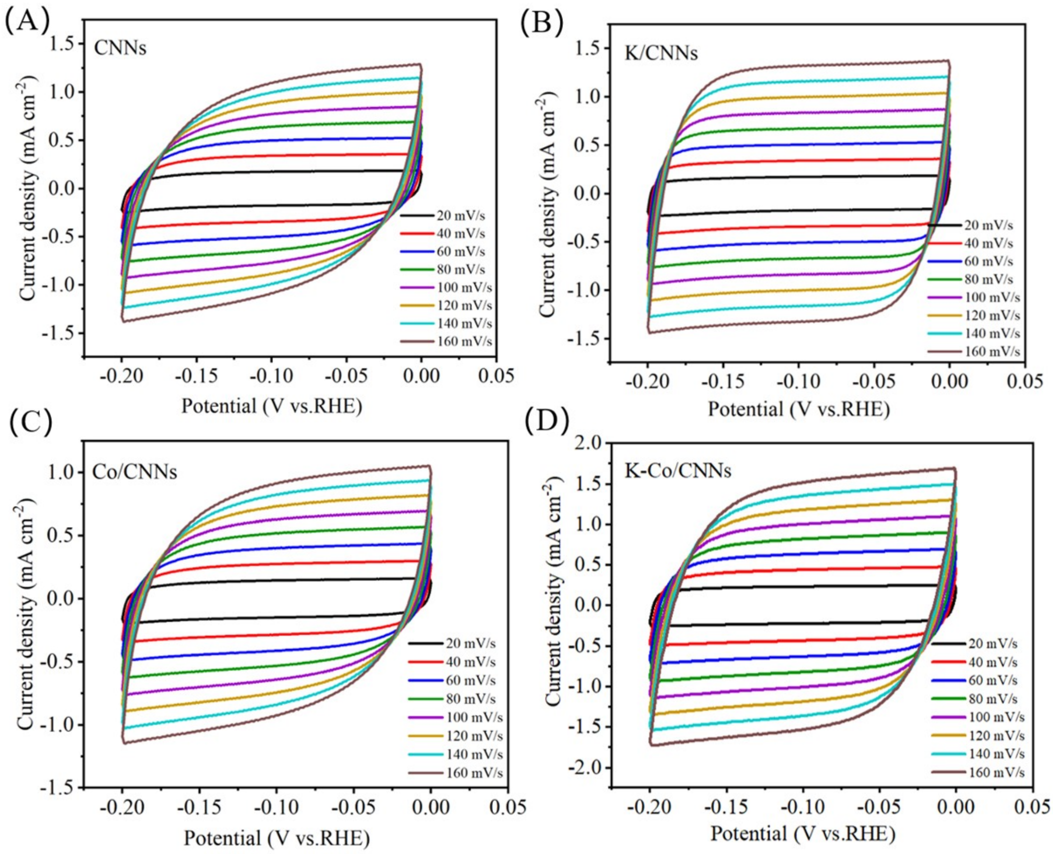

Figure S3. (A) (B) (C) (D) CV curve of CNNs, K/ CNNs, Co/ CNNs, K-CO / CNNs.

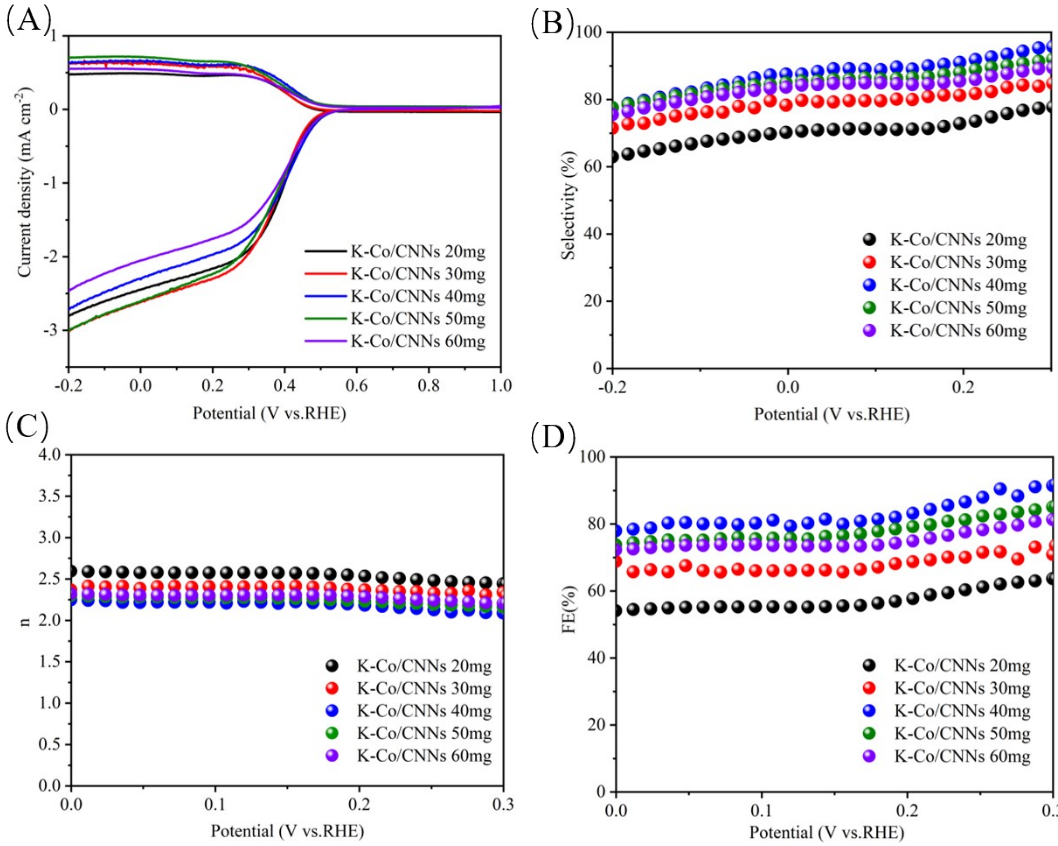

Figure S4. The different Co contents of the (A) LSV curve, (B) production rate of H_2O_2, (C) electron transfer number, (D) Faraday efficiency.

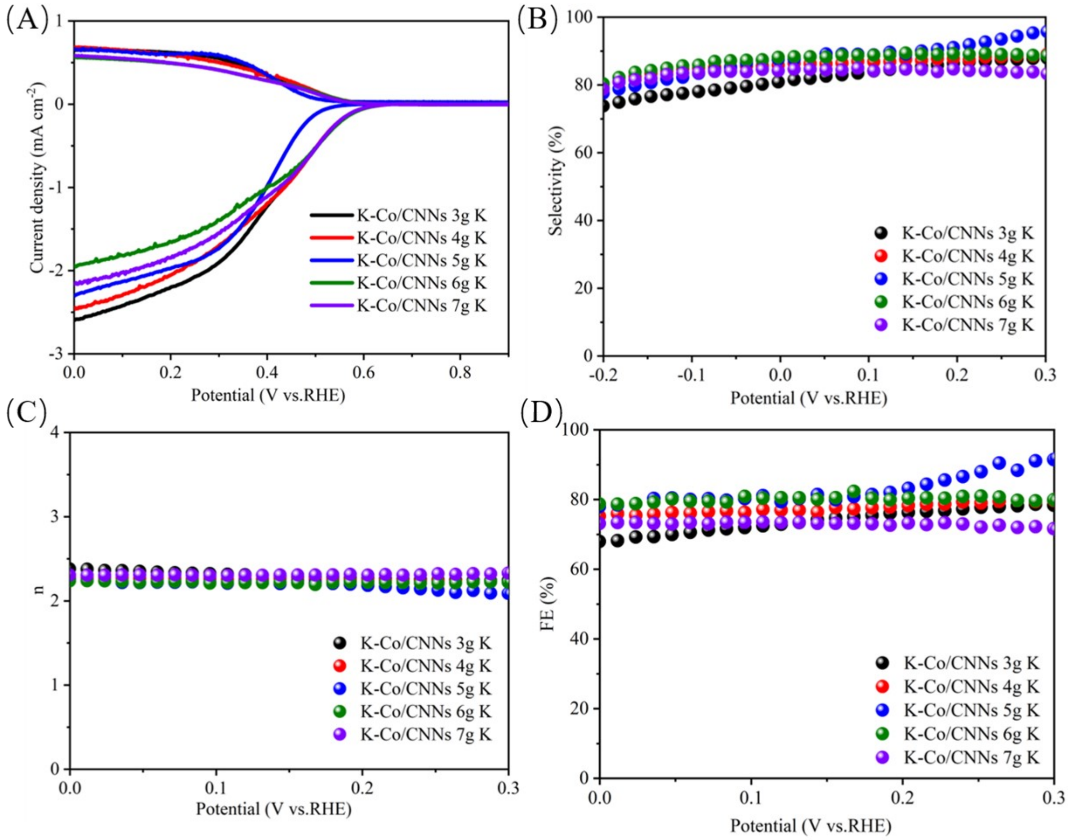

Figure S5. The different K contents of the (A) LSV curve, (B) production rate of H_2O_2, (C) electron transfer number, (D) Faraday efficiency.

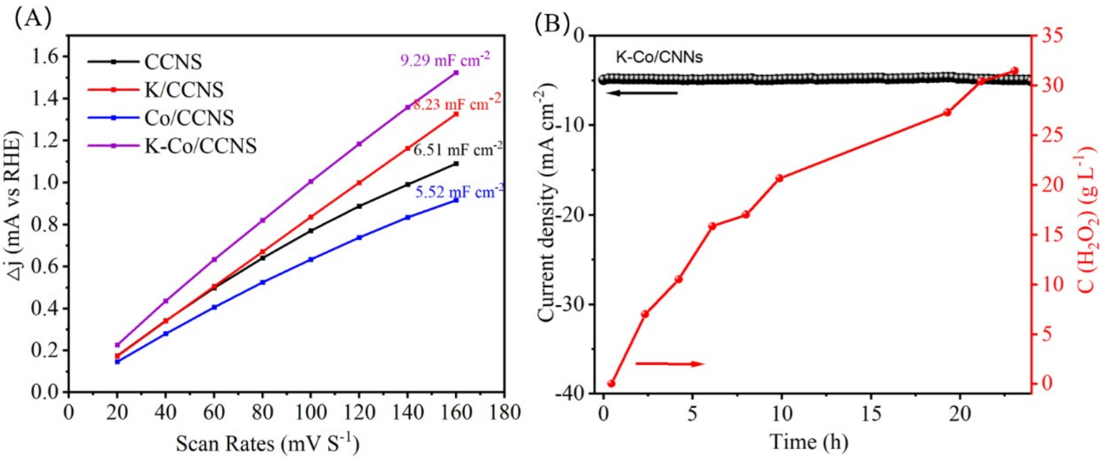

Figure S6. (A) CdI curve of CNNS, K/CNNS, Co/CNNS, K-CO /CNNS. (B) the accumulation of H_2O_2 within 24 hours of K-CO /CNNS.

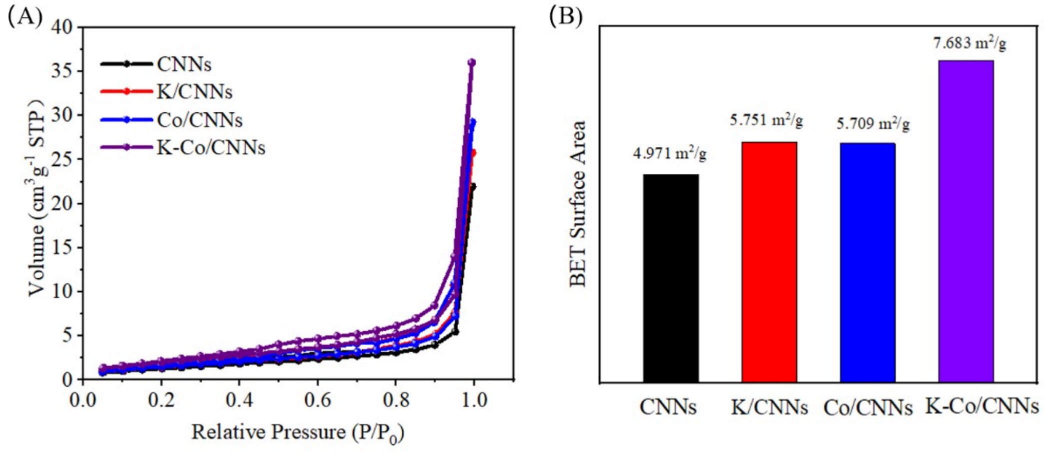

Figure S7. CNNs, K/CNNs, Co/CNNs and K-Co/CNNs of the (A) Comparison of N_2 adsorption and desorption curves, (B) Comparison of BET specific surface area.

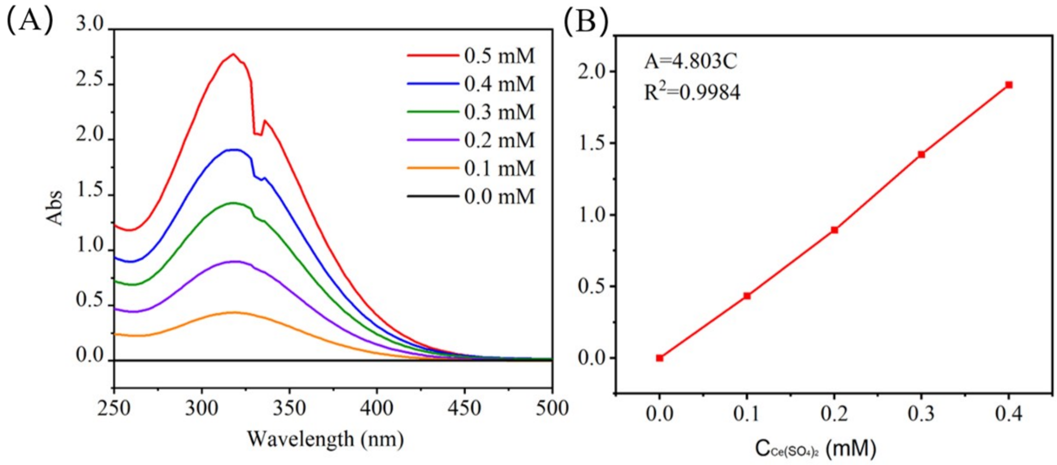

Figure S8. (A)The absorption spectra of different concentrations of $Ce(SO_4)_2$, (B) the linear relationship between the concentration of $Ce(SO_4)_2$ and the absorbance.

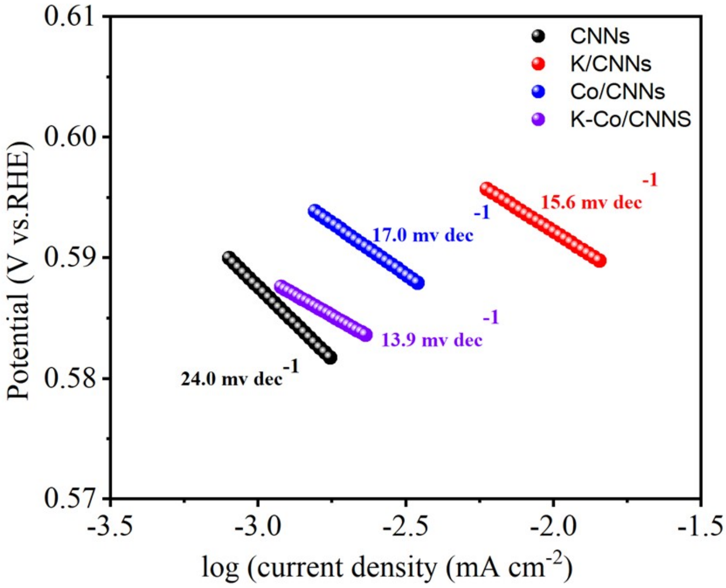

Figure S9. Tafel plots of CNNS, K/CNNS, Co/CNNs, K-Co/CNNs.

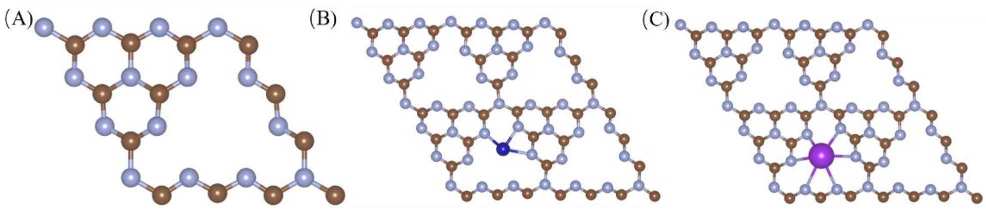

Figure S10. (A) Structural diagram of CNNs, (B) Structural diagram of Co/CNNs, (C) Structural diagram of K/CNNs.

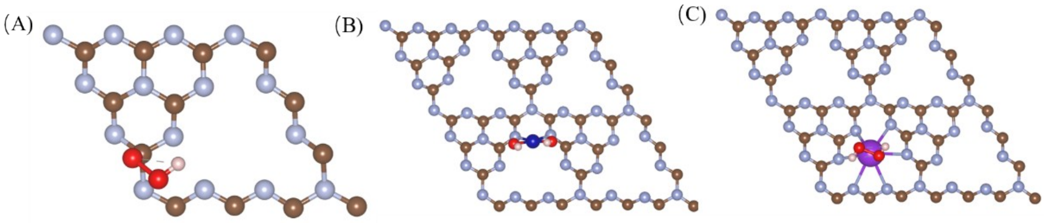

Figure S11. (A) Structure of CNNs for H_2O_2 adsorption, (B) Structure of Co/CNNs for H_2O_2 adsorption, (C) Structure of K/CNNs for H_2O_2 adsorption.

Table S1. The comparisons of different electrocatalysts towards two-electron ORR to produce H_2O_2.

Catalyst	Electrolyte	Selectivity	Ref.
K-Co/CNNs	0.1 M PBS (PH=7)	~97% (0.3 V_{RHE})	This work
Co/CNNs	0.1 M PBS (PH=7)	~87% (0.3 V_{RHE})	This work
K/CNNs	0.1 M PBS (PH=7)	~71% (0.3 V_{RHE})	This work
CNNs	0.1 M PBS (PH=7)	~76% (0.3 V_{RHE})	This work
MNCs	0.5 M H_2SO_4 （PH=0）	~90% (0.1V_{RHE})	1
Rh 1 /NC	PBS (PH=7)	~100%	2
Ni_3B	bicarbonate	~90% (0.3 V_{RHE})	3
c-WO_3	0.1M KOH (PH=13)	90%	4
Cr -ABIm	-	65%	5
r Ni@rGO	0.1M KOH(PH=13)	89%	6
o-$CoSe_2$	0.05M H_2SO_4	＞80%	7

FeC-O	0.1M KOH(PH=13)	95%	8
c-WO_3	0.1M KOH (PH=13)	90%	9
Pd/C	-	95.1%	10
$CoSe_2$	0.5 M H_2SO_4 （PH=0）	92%	11
Ni@B/N-CNTs-MS	0.1M KOH (PH=13)	~90%	12
NC-Ag/NHCS	0.5 M H_2SO_4 （PH=0）	89%–91%	13
$NiNb_2O_6$	0.1M KOH (PH=13)	96%	14
Pd-Zn	-	90.0%	15
MoO_{3-x}	0.1M KOH (PH=13)	93%	16
c-Mo/NCP	0.1 M PBS	77–85%	17
$MoSe_2$−MnP	0.1M KOH (PH=13)	97−98%	18
TM SA/CNNS	0.1 M PBS	98%	19

Table S2. Comparison of direct anthraquinone and oxygen reduction reaction methods for the preparation of H_2O_2.

	Indirect anthraquinone method	This work
yield	Stable hydrogenation efficiency above 11 g/L	31.7 g/L/24h
costs	Pd noble metal catalysts: expensive and scarce raw materials	Transition metal-based materials: high chemical stability, cost advantages and electrocatalytic activity comparable to noble metals
harmful byproducts	Organic impurities in the product	H_2O
Synthesis method	There are four processes: hydrogenation, oxidation, extraction and post-treatment	Simple two-step synthesis
security	Organic solvents are flammable and explosive	High security

REFERENCES

1. Park, J.; Nabae, Y.; Hayakawa, T.; Kakimoto, M.-a., Highly Selective Two-Electron Oxygen Reduction Catalyzed by Mesoporous Nitrogen-Doped Carbon. *ACS Catalysis* **2014,** *4* (10), 3749-3754.
2. Chen, J.; Ma, Q.; Zheng, X.; Fang, Y.; Wang, J.; Dong, S., Kinetically restrained oxygen reduction to hydrogen peroxide with nearly 100% selectivity. *Nature Communications* **2022,** *13* (1).
3. Kelly, S. R.; Shi, X.; Back, S.; Vallez, L.; Park, S. Y.; Siahrostami, S.; Zheng, X.; Nørskov, J. K., ZnO As an Active and Selective Catalyst for Electrochemical Water Oxidation to Hydrogen Peroxide. *ACS Catalysis* **2019,** *9* (5), 4593-4599.
4. Chen, L.; Chen, C.; Yang, Z.; Li, S.; Chu, C.; Chen, B., Simultaneously Tuning Band Structure and Oxygen Reduction Pathway toward High-Efficient Photocatalytic Hydrogen Peroxide Production Using Cyano-Rich Graphitic Carbon Nitride. *Advanced Functional Materials* **2021,** *31* (46).
5. Zhang, H.; Wang, Z.; Wang, Z.; Wang, L.; Wang, Y., Valence State Modulation of Chromium in Selective Hydrogen Peroxide Production Electrocatalysts. *ACS Applied Energy Materials* **2021,** *4* (9), 10114-10123.
6. Nosan, M.; Strmčnik, D.; Brusko, V.; Kirsanova, M.; Finšgar, M.; Dimiev, A. M.; Genorio, B., Correlating nickel functionalities to selectivity for hydrogen peroxide electrosynthesis. *Sustainable Energy & Fuels* **2023,** *7* (9), 2270-2278.
7. Sheng, H.; Janes, A. N.; Ross, R. D.; Kaiman, D.; Huang, J.; Song, B.; Schmidt, J. R.; Jin, S., Stable and selective electrosynthesis of hydrogen peroxide and the electro-Fenton process on CoSe2 polymorph catalysts. *Energy & Environmental Science* **2020,** *13* (11), 4189-4203.
8. Jiang, K.; Back, S.; Akey, A. J.; Xia, C.; Hu, Y.; Liang, W.; Schaak, D.; Stavitski, E.; Norskov, J. K.; Siahrostami, S.; Wang, H., Highly selective oxygen reduction to hydrogen peroxide on transition metal single atom coordination. *Nat Commun* **2019,** *10* (1), 3997.
9. Jiang, H.; Wang, Y.; Hu, J.; Shai, X.; Zhang, C.; Le, T.; Zhang, L.; Shao, M., Phase regulation of WO3 for highly selective oxygen reduction to hydrogen peroxide. *Chemical Engineering Journal* **2023,** *452*.
10. Lee, S.; Jeong, H.; Chung, Y.-M., Direct synthesis of hydrogen peroxide over Pd/C catalyst prepared by selective adsorption deposition method. *Journal of Catalysis* **2018,** *365*, 125-137.
11. Ji, Y.; Liu, Y.; Zhang, B.-W.; Xu, Z.; Qi, X.; Xu, X.; Ren, L.; Du, Y.; Zhong, J.; Dou, S. X., Morphology engineering of atomic layer defect-rich CoSe2 nanosheets for highly selective electrosynthesis of hydrogen peroxide. *Journal of Materials Chemistry A* **2021,** *9* (37), 21340-21346.
12. Xu, H.; Zhang, S.; Zhang, X.; Xu, M.; Geng, J.; Han, M.; Zhang, H., Melamine sponge templated synthesis of nickel nanoparticles encapsulated in B, N co-doped carbon nanotubes towards the selective electrosynthesis of hydrogen peroxide. *Journal of Materials Chemistry A* **2023,** *11* (19), 10204-10212.

13. Jin, M.; Liu, W.; Sun, J.; Wang, X.; Zhang, S.; Luo, J.; Liu, X., Highly dispersed Ag clusters for active and stable hydrogen peroxide production. *Nano Research* **2022,** *15* (7), 5842-5847.
14. Liu, C.; Li, H.; Chen, J.; Yu, Z.; Ru, Q.; Li, S.; Henkelman, G.; Wei, L.; Chen, Y., 3d Transition-Metal-Mediated Columbite Nanocatalysts for Decentralized Electrosynthesis of Hydrogen Peroxide. *Small* **2021,** *17* (13).
15. Wang, S.; Gao, K.; Li, W.; Zhang, J., Effect of Zn addition on the direct synthesis of hydrogen peroxide over supported palladium catalysts. *Applied Catalysis A: General* **2017,** *531*, 89-95.
16. Jiang, H.; Zhang, C.; Wang, Z.; Zhang, Y.; Le, T.; Mei, Y.; Feng, Y.; Hu, J., Enhanced two-electron oxygen reduction for hydrogen peroxide production via fine-tuning the concentration of oxygen vacancies in MoO. *Applied Catalysis A: General* **2023,** *661*.
17. Jin, M.; Liu, S.; Meng, G.; Zhang, S.; Liu, Q.; Luo, J.; Liu, X., Low-Coordinated Mo Clusters for High-Efficiency Electrocatalytic Hydrogen Peroxide Production. *Advanced Materials Interfaces* **2022,** *10* (1).
18. Kagkoura, A.; Stangel, C.; Arenal, R.; Tagmatarchis, N., Molybdenum Diselenide–Manganese Porphyrin Bifunctional Electrocatalyst for the Hydrogen Evolution Reaction and Selective Hydrogen Peroxide Production. *The Journal of Physical Chemistry C* **2022,** *126* (35), 14850-14858.
19. Yang, H.; Ma, F.; Lu, N.; Tian, S.; Liu, G.; Wang, Y.; Wang, Z.; Wang, D.; Tao, K.; Zhang, H.; Peng, S., Transition metal single atom-optimized g-C(3)N(4) for the highly selective electrosynthesis of H(2)O(2) under neutral electrolytes. *Nanoscale Horiz* **2023,** *8* (5), 695-704.